EXPERIMENTAL TESTS AND FINITE ELEMENT ANALYSES OF THE DEMOUNTABLE STEEL TRUSS JOINTS WITH RECTANGULAR HOLLOW SECTIONS

ABDULLAH AL-MAISARI, NEWTON AVILA DOS SANTOS, MIKI SALLI & ZHONGCHENG MA
Häme University of Applied Sciences, HAMK Tech Research Unit, Finland

ABSTRACT

An innovative demountable solution for the steel roof trusses with rectangular hollow sections (RHS) was developed to promote the reuse of steel roof trusses. Self-drilling screws were used for the RHS truss joints to replace the traditional welded solution. The drillability of screwed connections for S355 and S500 steel plates was tested in terms of drilling time and failed attempts. The effects of the size of pilot holes and the type of screws were studied. Lap-shear behaviour and strength with varying gap distances between the plates were also studied experimentally. Finally, three T-joint tests in tension were executed to investigate the load-carrying capacity of the joints. Digital image correlation technique was used to record the deformation of joint area. Finite element analyses were firstly performed for the lap-shear tests using simplified modelling methods. Then, the simplified modelling method of the screwed connection was validated by the T-joint tests.

Keywords: demountable joint, RHS, self-drilling screws, drillability, lap-shear behaviour, T-joint.

1 INTRODUCTION

The roof truss structure with rectangular hollow sections (RHS) has been widely used in Nordic countries, especially in Finland. The tubular chords and braces are welded together to form the structures. The design of truss joints with welded RHS is well specified by EN 1993-1-8.

In recent years, the demountable solutions for RHS truss joints attract the research and innovations. Non-weld truss joints are very common in cold-formed steel truss structures with open sections. Screw connection, bolt connection, press-joining connection, and rosette connection are typical applications [1]–[3]. However, the demountable solutions of non-weld RHS truss joint is very challenging since the inner surface of RHS is inaccessible. With the advent of laser cutting technology, the complex shape of cutting can be easily made, the truss joint can be made by plug and play contact without welding [4]–[6].

The use of modern 3D laser cutting technology enables easy and precise cutting in steel elements including enclosed RHS. The shape of the cutting can be very complex and easily controlled. In the developed non-welded RHS truss joints by Szlendak and Szpyrka for tension braces [4], forces are transferred only by bearing and shearing stresses in the elements in contact with each other, the key (bracing elements) and the lock (holes in the chord). Due to lack of permanent connections between the elements, such structure can be dismantled and reassembled elsewhere.

A demountable joint for tubular sections using tab–slot configuration without welds and screws was patented by Iriarte [7]. The cuts and slots can be made by laser cutting or plasma cutting. However, the perceived strength of the joint for building truss application may be too weak to resist the tensile and compression forces in the braces.

In this paper, a novel demountable solution for RHS trusses using self-drilling screws and computer numerical control (CNC) cutting process is developed and the drillability and mechanical behaviour are investigated both experimentally and numerically. The mechanical tests include lap-shear tests and T-joint tests.

WIT Transactions on The Built Environment, Vol 216,
www.witpress.com, ISSN 1743-3509 (on-line)
doi:10.2495/HPSM250051

2 DRILLABILITY TESTS

Drillability of self-drilling screws refers to the ability of a screw to penetrate and fasten into a material efficiently or without failure. It is influenced by factors such as: the diameters of pre-drilled holes, the length of the drilling bits of screws, plate material hardness, and rotational speed and torque. The purpose of drillability tests is to find out the influence of these parameters on the drilling times and successful attempts. Prior to this drillability study, the truss joints with pilot holes were cut using laser cutting. However, nearly all drilling attempts failed due to the laser hardening effect along the edges of round holes. To address this issue and further investigate the drillability, pilot holes were mechanically drilled instead of using laser cutting in this study.

Self-drilling screws are typically used to fasten a thin sheet (max. 2 mm) made from S280GD up to S550GD to a thicker substructure made of structural steel grade up to S355. Drilling capacities of these screws increase as the screw diameter increases but is usually less than 6 mm. The long drill bit versions might be able to drill through 13.5 mm thick plates. The European Technical Assessment (ETA) for these screws usually only include design situations in which thin sheets are being attached to thicker substrates. Therefore, it is important to find out how these screws perform with thicker plates that might also be made from high-strength steel. The effect of small gaps between plates on the drillability needed to be investigated as well. Moreover, the quantitative effects of the diameters of pilot holes on the drilling times and successful attempts need to be further studied.

2.1 Test method and cases

The test objective is to investigate how self-drilling screws with ordinary and long drill bits work with 4 mm and 8 mm thick steel plates made from S355 and S500 when there is a small 1–2 mm gap between the plates to be connected. The test variables that affect the outcome of the tests are pilot hole size, drilling speed, plate thicknesses, plate material, screw size, screw type, gap size, and drilling maximum torque. The screw options for the tests are shown in Fig. 1.

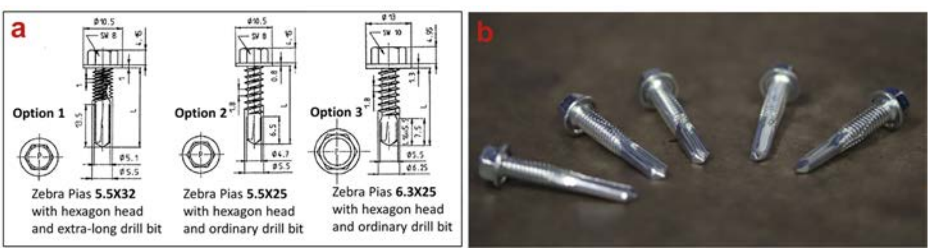

Figure 1: (a) Screw options; and (b) PIAS 5.5 × 32 with a long drill bit.

Testing has been implemented by manufacturing the test specimens which consist of a pair of plate pieces (Fig. 2) that have been fixed together utilizing small bolts. In test cases with a gap between the plates, 1 mm thick washers have been added to produce the desired gaps between two steel plates. Pilot holes of varying size have been pre-drilled to the plates. Pilot hole sizes 3.5 mm, 4.0 mm and 4.5 mm as well as the case without pilot holes have been investigated with three different screw options. Plates were fixed by a bench vice, and screws were driven to the plates using a battery-operated drill. Drilling times were recorded in six attempts in each case.

Figure 2: Example of (a) test specimen with screws drilled in; and (b) drillability test assembly pair of plates (4 + 8 mm plates with 1 mm gap).

There are 144 different test cases. To investigate the torque and the drilling time, each case is repeated nine times. This means driving 1,296 screws into the plates. In addition to these tests, also drilling speed (measured in revolutions per minute (RPM)) effect has been studied to select a suitable RPM for the tests. The preliminary study for the drilling speed has been done for S355 and S500, 8 + 4 mm plates without pilot holes to demonstrate an extreme situation.

2.2 Test results

RPM tests showed that the optimal drilling speed is 1400 rpm for 8 mm thick S500 plates and 1700 rpm for S355 plates. High speed combined with moderate push force and a high strength steel (HSS) substrate produce excessive heat which limits drill bit endurance in thicker HSS material. Drillability performance was improved with thinner plates and pre-made pilot holes. The Milwaukee ONEDD3 drill was used, with torque settings up to 158 (Nm).

Tests on screw options 1, 2, and 3 (as shown in Fig. 1(a)) revealed that screws with longer drill bits performed well for both S355 and S500 plates. However, for thicker 8 mm plates, especially without properly sized pilot holes, a reduced drilling speed was necessary for success. It was found that screws with standard drill bits frequently failed due to the exceedance of their drilling capacity. Pre-made pilot holes significantly reduced drilling time and improved success rates. Figs 3 and 4 present the average drilling times and failure rates for PIAS 5.5 × 32 screws with long drill bits in S355 and S500 plates, respectively.

3 LAP SHEAR AND T-JOINT TESTS

Force transfer between the brace members and the chord member in a mechanical truss joint is based on a shear force transfer mechanism. Joint forces are transferred between the plate walls of the tubular profiles by the screw connectors. This behaviour can be mimicked in simple lap shear tests. Tests are carried out to obtain information on the strength and deformation of axially loaded single lap connections of steel plates with self-drilling screws and a possibility of a small gap between the connected plates.

3.1 Description of lap-shear tests

Test assemblies for the lap shear tests (Fig. 5) are composed of pairs of plates with a size of 60 mm × 300 mm. The thicknesses of the plates are 4 mm and 8 mm, respectively and made

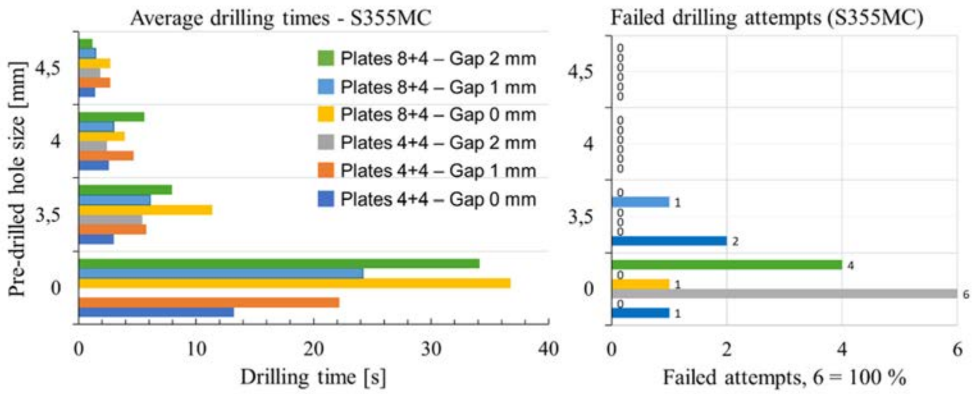

Figure 3: Drillability test results for PIAS 5.5 × 32 screws in S355 plates.

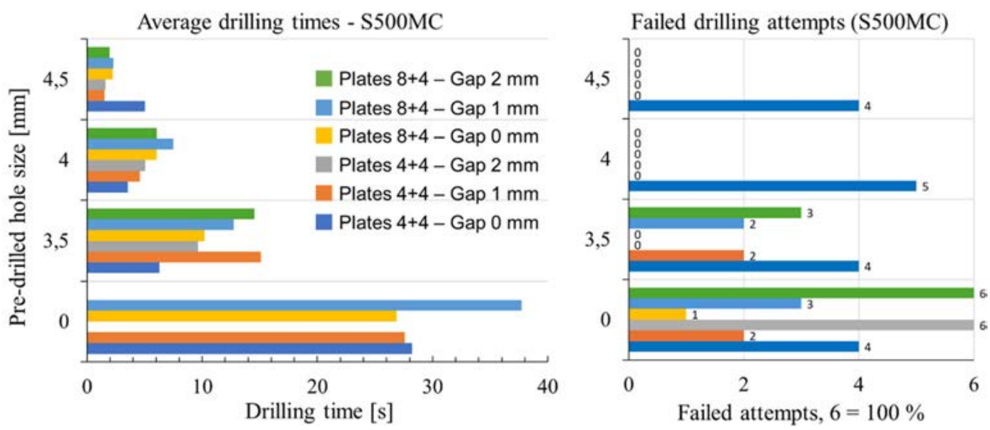

Figure 4: Drillability test results for PIAS 5.5 × 32 screws in S500 plates.

from steel grades S355MC and S500MC. To eliminate gripping problems with the 50 kN tensile testing machine, the ends of the test plates are grinded to bare steel. Four holes for M4 fixing bolts are drilled before the self-drilling screw is added. The bolts are removed once the test assembly has been gripped to the tensile testing machine.

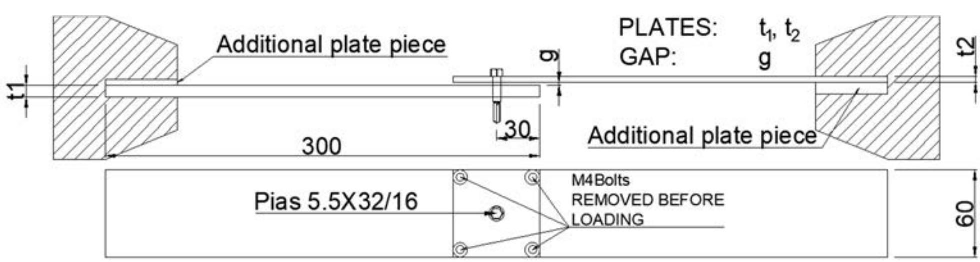

Figure 5: Lap shear test assembly.

WIT Transactions on The Built Environment, Vol 216, © 2025 WIT Press
www.witpress.com, ISSN 1743-3509 (on-line)

End distance (e_1) and edge distance (e_2) of the connection are chosen so that they do not reduce the bearing strength of the connection. For self-drilling screws, the nominal diameter of the screw can be used for a conservative approximation. Gaps are created using 1 mm washers, and additional (filler) plates in the ends are added to eliminate setup eccentricity as shown in Fig. 5.

Screw option 1 (ZEBRA Pias 5.5 × 32) was selected for the lap shear tests due to its strong performance in drillability tests. As shown in Table 1, a total of 36 tests were conducted across 12 test series, with each series consisting of three individual tests. The tests were performed on single fasteners while varying key parameters: plate thickness (4 + 4 mm/ 8 + 4 mm), plate gap (0 mm/1 mm/2 mm), and steel grade (S355MC/S500MC). Testing was displacement-controlled at 0.2 mm/min, using extensometer sensor arms for strain measurement and a load cell for force measurement. The extensometer gauge length was set to 100 mm.

Table 1: Lap shear test results.

Lap shear test cases	Steel grade	Average shear strength (kN)
4 + 4 mm Plates, Gap = 0 mm	S 355 MC	10.93
8 + 4 mm Plates, Gap = 0 mm		10.20
4 + 4 mm Plates, Gap = 1 mm		9.34
8 + 4 mm Plates, Gap = 1 mm		8.92
4 + 4 mm Plates, Gap = 2 mm		8.31
8 + 4 mm Plates, Gap = 2 mm		8.04
4 + 4 mm Plates, Gap = 0 mm	S 500 MC	10.62
8 + 4 mm Plates, Gap = 0 mm		10.70
4 + 4 mm Plates, Gap = 1 mm		9.69
8 + 4 mm Plates, Gap = 1 mm		9.16
4 + 4 mm Plates, Gap = 2 mm		8.81
8 + 4 mm Plates, Gap = 2 mm		8.31

3.2 Results of lap-shear tests

Table 1 lists the measured average shear strength for lab-shear tests for different steel grades, plate thicknesses and gap dimensions. The pre-drilled hole in all the tests was 4.0 mm in diameter and the screw type was Pias 5.5 × 32. The average shear strength for screws was the average out of three successful tests.

As shown in Table 1 and Fig. 6, the gap effect on the shear strength of the screw is quite considerable in both steel grades S355MC and S500MC. The shear strength of 5.5 × 32 screw dropped about 30% in the case of S355MC and 20% in the case of S500 MC steel plates with the increasing gap distances from zero to 2 mm. The average shear strength is not affected significantly between grades S355MC and S500MC plates both with and without a gap. The elastic stiffness of the lap-shear joint for S500 plates is higher than S355 plates without a gap while remains similar for those with 2 mm gap. Ductility is slightly higher in the case of 2 mm gap compared to zero gap between plates. However, the overall behaviour of lap-shear joints demonstrates brittle failures.

For the 8 + 4 mm plate case with S355 steel (Fig. 7), the ultimate shear strength decreased by approximately 7% compared to the 4 + 4 mm plates for the cases with zero gap. This reduction may be attributed to the larger engagement area (12 mm) between the screw thread

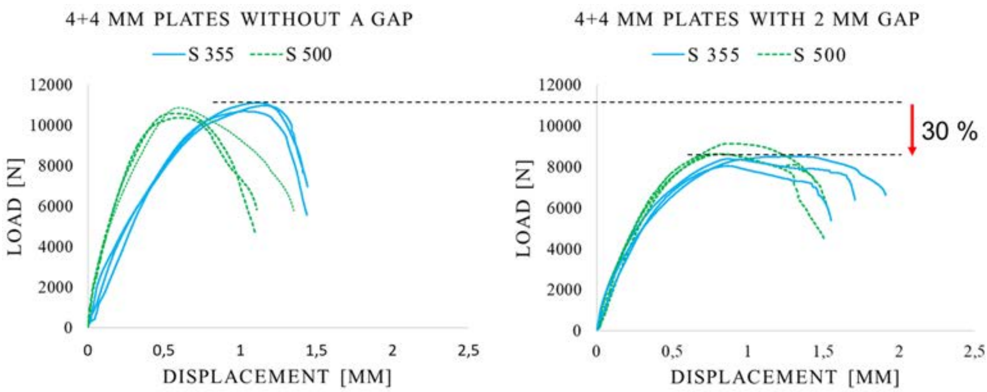

Figure 6: Comparison of lap shear test results for 4 + 4 mm plates with and without gaps for different steel grades.

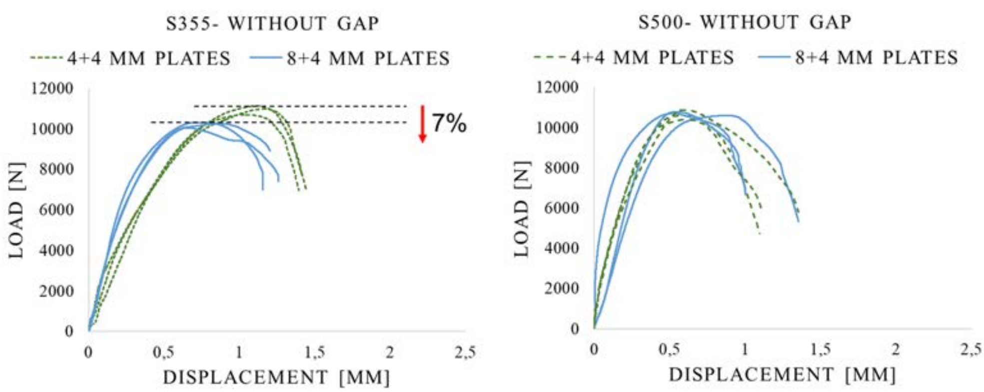

Figure 7: Comparison of lap shear test results for different steel grades and plate thickness arrangements without gaps.

and the plates. However, in the case of S500 steel, the shear strength for the 8 + 4 mm plates remained nearly the same as for the 4 + 4 mm plates. This was the only instance where the 4 + 8 mm plate arrangement did not negatively impact shear strength. In all other test configurations, the 4 + 8 mm plates resulted in a shear strength reduction of 3.3% to 7.15% depending on the gap distances.

In these tests, the plate arrangement consistently followed the sequence of the 8 mm plate first, followed by the 4 mm plate. The 8 mm plates were drilled first, as the thicker chord members are typically drilled before the braces in the construction of steel trusses for this type of demountable mechanical joint solution.

As shown in Fig. 8, the primary failure mode observed was shear failure of the screw, with the fracture plane aligning parallel to the sliding surfaces. As expected, the plates remained less deformed due to their higher bearing strength. Prior to failure, the screw exhibited gradual slight tilting under load before ultimately shearing failure.

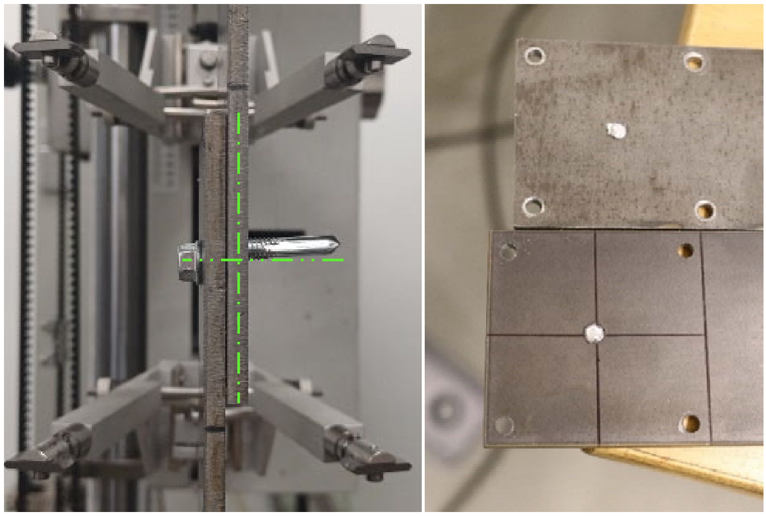

Figure 8: Shear failure of screw – lap-shear test.

3.3 Description of T-joint tests

The purpose of the T-joint tests in this study was to evaluate the influence of screw spacing distances on the stiffness and load-bearing resistance of demountable mechanical joints under tension load. The shear strength of the demountable T-joint solutions was derived from lap shear test results. Fig. 9 shows the test specimen and setup for T-joint test in tension. The cases reported in this paper are part of a more comprehensive test program which will be carried out shortly later.

For specimen assembly, steel tubes are cut to a length of 600 mm. A total of 24 predrilled 4.0 mm holes are created, followed by the installation of 12 Pias 5.5 × 32 screws on each side of the chord. Table 2 shows the details of the T-joint test cases.

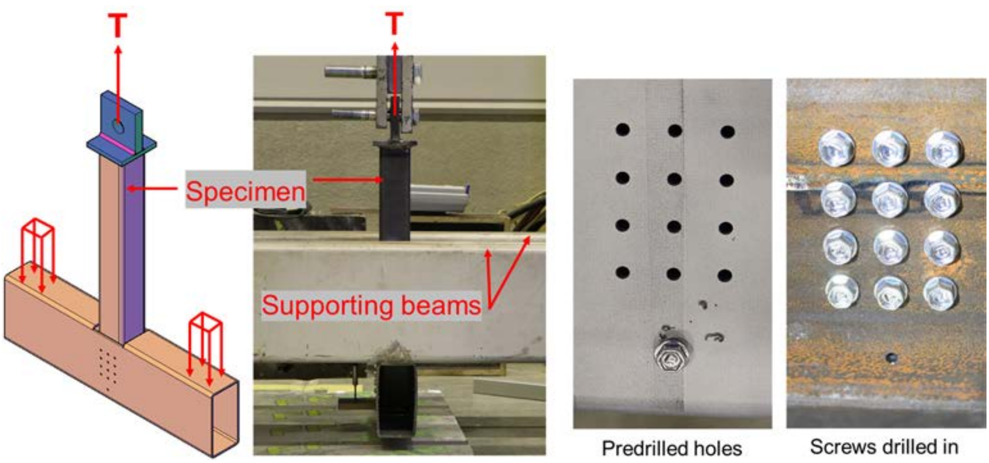

Figure 9: Test specimen and setup for T-joint tests.

Table 2: T-joint test cases in tension.

Case	Chord section	Brace section	Screws spacing (mm)	No. of screws per side	Steel grade	Predrilled hole size (mm)
4	RHS 160X80X4	SHS 70X70X4	15	12	S420	4.0
5			20			
6			25			

The end distance (e_1) and edge distance (e_2) of the connection are done according to EN 1993-1-8, $e_1 \geq 3d_0$ and $e_2 \geq 1.5d_0$, where d_0 is the screw hole diameter. The number of screws is determined based on the estimated shear resistance of the screws.

The tests were displacement-controlled at a loading rate of 0.8 mm/min, utilizing a tensile frame with a capacity of 250 kN. Digital image correlation (DIC) was employed to precisely capture the full-field strain distributions across the joint. In addition, a linear variable differential transformer (LVDT) sensor was installed to measure the relative displacements between the brace and chord member. For DIC analysis, the chord member with the gap between the chord and brace (identified as the weaker component) was speckle-painted to facilitate DIC strain tracking.

3.4 Results of T-joint tests

As illustrated in Fig. 10, the screws exhibited pure shear failure under loading. Minor bending of screw shanks was observed in some cases. Additionally, localized deformations occurred at the chord holes due to bearing stresses from the screws. Variations in hole bearing deformation were observed after removing the failed screws and attributed to the misalignment between brace and chord holes due to the manufacturing tolerances and drilling issues.

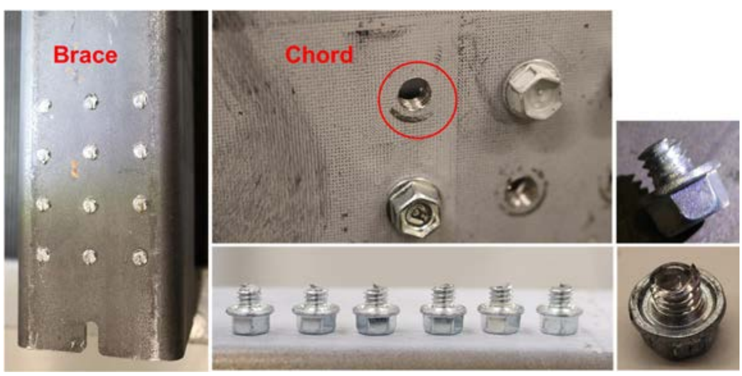

Figure 10: Failure modes.

The ultimate shear strength for T-joint test cases 4, 5 and 6 were 217.02, 225.09 and 229.82 kN, respectively. As shown in Fig. 11, the results revealed that screw spacing has obvious influences on the shear resistance: a 25 mm spacing increased average shear strength by 6% compared to a 15 mm spacing. Moreover, ductility increased by about 30% in case 6 with 25 mm spacing compared to case 4 with only 15 mm spacing.

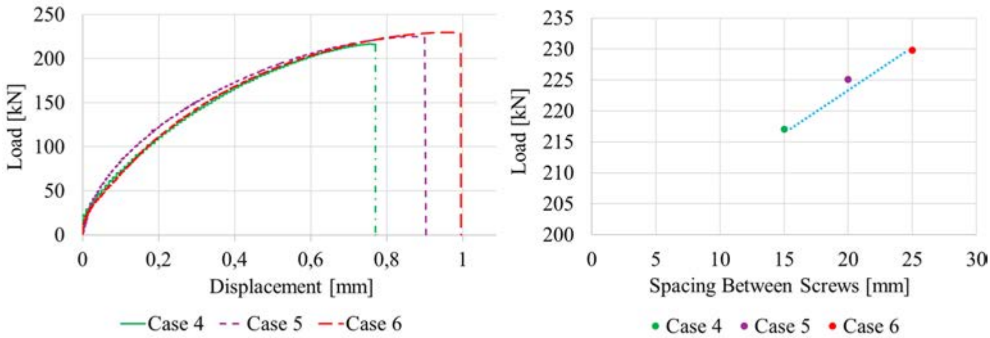

Figure 11: (Left) Load versus displacement curves for T-joint tests; and (Right) Effect of spacing on shear strength of T-joints.

Additionally, it was found that the average shear strength of single screws in the group decreases compared to lap-shear test results. The reduction is probably due to the rigidity of the joint since rotation of screws is prevented and the gap between brace and chord walls in one side. While some screws were drilled twice during assembly, it may have minor effect on joint performance. However, minor hole misalignment caused by machining tolerances led to slightly uneven bearing resistance across holes, which may also explain some challenges during assembly.

The use of LVDTs proved inadequate for capturing precisely the relative displacements between the brace and chord. To improve the instrumentation of the tests, strain gages will be implemented in future tests to validate the DIC measurement.

4 FE ANALYSYS

4.1 FE models

Multiple finite element (FE) analyses were performed using ABAQUS/Explicit software and the models were validated by the lap shear and the T-joint experimental tests. Nonlinear geometric and material behaviours were incorporated into the numerical models. The steel plates of both lap shear and T-joint tests were modelled with S420 steel grade and elasto-plastic material properties obtained from the literature [8]. The yield strength, ultimate stress, and Young's modulus applied to the numerical models were 518.46 MPa, 567.93 MPa, and 210 000 MPa, respectively. The mechanical properties, originally represented as engineering stress–strain curves, were converted into trues stress and effective plastic strain curves.

The lap shear experiments were carried out on S355 and S500 steel plates whereas S420 tubular sections were utilized for all T-joint experiments. Therefore, the lap shear experimental results of S355 and S500 plates were interpolated to obtain the results of S420 plates and further used for the FE models' validation.

ABAQUS connector elements were used to model the screws. Three-dimensional eight-node solid hexahedral elements (C3D8) were employed to model the full geometry of the steel plates in the numerical analyses for both lap shear joints and T-joints. A refined mesh was used around the screw holes to capture local stress concentrations, while a coarser mesh was employed for the areas away from these critical areas aiming to optimize computational efficiency. Boundary conditions in the numerical analyses mirrored the experimental test setups. In these explicit analyses, general interactions including a friction coefficient of 0.1 were defined between contacting steel sheets.

4.1.1 Lap shear tests validation

The lap shear experimental tests were validated in two phases. On the first phase a connector alone was validated whereas on the second phase the lap shear tests including the plates geometry was validated.

A bushing connector, which allows the definition of both translational and rotational components of relative motion, was selected to numerically represent the behaviour of the screws. The end nodes of the connectors were coupled to the nodes on the respective walls of the screw holes. The interpolated S420 lap shear test results were utilized as input to define the nonlinear response of the connectors. The behaviour of the connectors included elastic stiffness, plastic deformation, damage initiation and evolution criteria modelled according to Abaqus manual.

Translational properties derived from the interpolated S420 lap shear tests were applied to the connector in directions transverse to the hole axis of symmetry. Along the screw axis, stiffness properties derived from a Young's modulus of 210,000 MPa and plastic properties based on the screw tensile strength specified by the manufacturer were applied. No restriction was imposed on rotation around the hole's symmetry axis itself. Fig. 12(a) illustrates a bushing connector and Fig. 12(b) shows the comparison between force–displacement curves obtained from the interpolated S420_G0_4+4 lap shear test and the corresponding numerical model consisting only of a bushing connector. The numerical model accurately predicts both force and displacement measurements from the lap shear experiments. Similar accuracy was obtained in all other numerical models employing only bushing connectors for lap-shear tests.

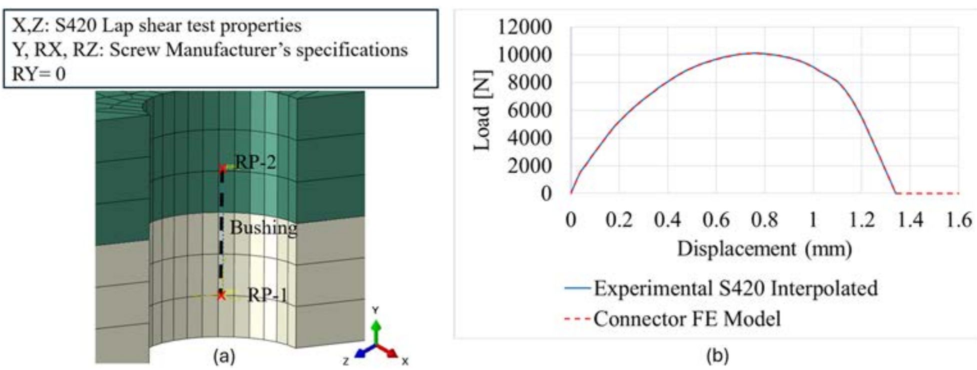

Figure 12: (a) Bushing connector; and (b) Connector and lap shear test force–displacement comparison.

For the validation of the complete lap shear tests, full geometry of the plates was modelled, and the screws were replaced by validated bushing connectors. Connector endpoints were attached to two distinct reference points located at the mid-thickness of the plates, on the centre of the screw holes (Fig. 12(a)). A forced displacement of 2 mm was applied to the end of one plate, while one end of the opposite plate was fixed, replicating experimental test setup. The original results obtained from numerical models indicated good agreement in ultimate load predictions but exhibited slightly lower stiffness compared to experimental results. This stiffness discrepancy likely arose from the neglected steel plate deformations and the simplifications introduced by replacing the screw with a connector.

To reduce these differences and better capture only the screw behaviour in the connector model, the stiffness of the connectors was refined through a reverse engineering approach in the lap shear model. Data points from FE models and experimental lap shear tests were collected at same load levels and the difference in displacements was computed. The additional displacements were subtracted from the connector model. The refined properties for the bushing connector were then applied for the lap shear models. Fig. 13(a) shows the lap shear FE model, while Fig. 13(b) compares experimental and numerical force–displacement curves for the S420_G0_4+4 test. The results indicate that the FE models can accurately capture the ultimate loads and stiffness in the lap shear model. Similar results were obtained in all other lap shear FE analyses. The derived connector properties will be used in the following T-joint FE analyses.

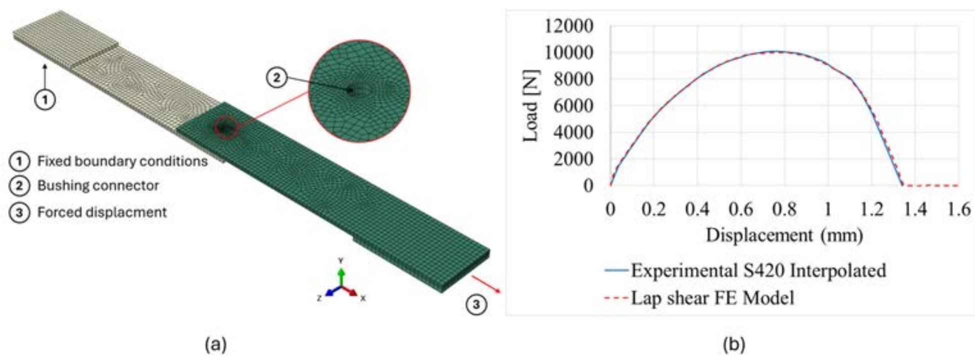

Figure 13: Lap shear. (a) Numerical model; and (b) Lap shear FE and experimental test force–displacement comparison.

4.1.2 T-joint validation

For numerical modelling of T-joints, the full geometry of the chord was modelled, while the vertical brace was represented with a shortened geometry to improve computational efficiency. The screws were modelled by the bushing connectors with properties validated by lap-shear tests. Fig. 14(a) shows the FE model for T-joint Case 06, and Fig. 14(b) presents experimental versus numerical force–displacement results. The numerical models demonstrated slightly lower initial stiffnesses and higher ductility in comparison with the experiments. It is important to note that, for the validation of T-joint FE models, interpolated connector properties for S420 plates were used instead of actual test data, which may have contributed to the observed discrepancy.

Table 3 summarizes the ultimate forces from experimental tests and numerical simulations, including the percentage differences. The numerical models were not able to accurately capture the spacing effect on ultimate load discussed in Section 3.

5 DISCUSSIONS AND CONCLUSIONS

The experimental part of this study involved three tests: drillability, lap-shear, and T-joint tests. Over 144 drillability tests showed that the optimal drilling speed is 1,400 rpm for S500 plates and 1,700 rpm for S355 plates. Drilling performance was improved with thinner plates

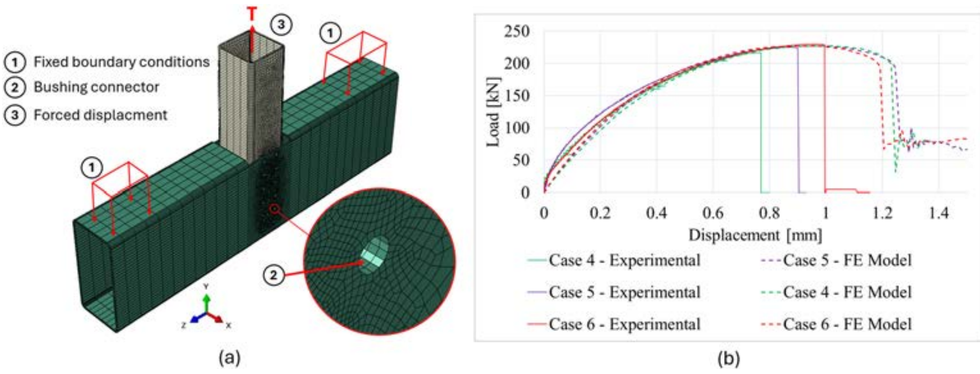

Figure 14: T-joint. (a) Numerical model; and (b) FE and experimental test force–displacement comparison.

Table 3: Ultimate force comparison between experiments and numerical models.

Cases	Experimental F_U (KN)	Numerical F_U (KN)	% Difference
04 Tension	217.02	227.22	4.5
05 Tension	225.09	227.37	1.0
06 Tension	229.82	227.23	1.2

and pre-made pilot holes. The Pias 5.5 × 32/16 screw performed best due to the length of drill bit. S500 plates required higher torque for successful drilling. With the increasing diameter of pilot holes from 3.5 mm to 4.5 mm, the drilling performance including drilling time and success rate has been improved. However, the effects of increasing pilot hole diameters on the mechanical behaviour of the joints need to be studied further.

The lap-shear tests showed that a gap distance from zero to 2 mm significantly reduces the shear strength, with a 30% drop in S355MC steel and 20% in S500MC. Ductility was slightly higher with a 2 mm gap than with zero gap. Plate arrangement also influenced the strength – 8 + 4 mm plates in S355 saw a 7% reduction, while in S500, shear strength remained unchanged. The primary failure mode was shear fracture of the screw, with slight tilting observed before failure. The plates remained less deformed, indicating that the screw bore the larger shear stresses before fracturing along the shear plane and the bearing stresses around the holes of the plates are relative smaller.

For T-joint tests, the screws failed in pure shear, with minor bending in some cases. Minor hole deformations occurred in some cases due to bearing stresses, varying in severity due to misalignment from manufacturing tolerances and drilling issues. Additionally, the T-joint tests showed that increasing screw spacing improves shear strength and ductility. Case 6 (25 mm spacing) had 6% higher shear strength and 30% greater ductility than Case 4 (15 mm spacing). Shear strength of average single screws in T-joint was lower than in lap-shear tests, likely due to joint rigidity preventing screw rotation and the gap between brace and chord walls in one side. Hole misalignments caused uneven bearing resistance but did not significantly impact the performance.

The numerical part of this study included three steps: connectors validation, lap shear tests validation and T-joint tests validation. The FE model composed of only a bushing connector accurately captured the behaviour of the experimental lap shear tests. However, stress/strain field around screw holes in the plates might differ from the reality when the bushing connectors replaced screws in complete lap shear and T-joint models. This indicates that, although using connectors in place of screw geometry provides a reasonable approximation of overall load-carrying behaviour, this simplification might not fully represent the stress/strain behaviour of steel plate around the screw holes. Therefore, further investigation is necessary to assess the suitability of employing this simplified approach, particularly for parametric studies.

ACKNOWLEDGEMENT

RFCS funding for DreamFAB project (grant number 101111547) is greatly acknowledged by the authors.

REFERENCES

[1] Zaharia, R. & Dubina, D., Stiffness of joints in bolted connected cold-formed steel trusses. *Journal of Constructional Steel Research*, **62**, pp. 240–249, 2015.
[2] Kaitila, O., Study on the behavior of a new light-weight steel roof truss. *Rakenteiden Mekaniika*, **31**(3–4), pp. 4–15, 1998.
[3] Pedreschi, R.F. & Sinha, B.P., The potential of press-joining in cold-formed steel structures. *Construction and Building Materials*, **10**(4), pp. 243–250, 1996.
[4] Szlendak, J.K. & Szpyrka, A., Resistance of tension brace in plug and play N shape RHS truss connection. *Journal of Civil Engineering, Environment and Architecture*, **65**(2/18), pp. 177–186, 2018.
[5] Szlendak J.K. & Oponowicz P.L., Experimental tests and numerical models of one and double side non-welded T RHS truss joints. *11th International Conference on Modern Building Materials, Structures and Technique*, Vilnius, 16–17 May, 2013.
[6] Szlendak, J.K., Resistance of laser made T RHS joints under compression load. *SDSS' Rio 2010 Stability and Ductility of Steel Structures*, Rio de Janeiro, Brazil, 8–10 Sep., 2010.
[7] Iriarte, C.G., Retaining system for joints. Patent number US20200011358. World Intellectual Property Organization (WIPO), 2022. https://patentscope.wipo.int.
[8] Yuce, C., Karpat, F., Yavuz, N. & Sendeniz, G., Designing for sustainability and reliability in an automotive seat structure. *Sustainability*, **6**(7), pp. 4608–4631, 2014.